Supplementary Materials

Manuscript Title: Synergistic anionic and cationic co-doping in cobalt hydroxide for enhanced hydrogen production coupled with urea electrooxidation

Manuscript Author:
Shahid Khan[#], Yafei Feng[#], Yanxu Chen[#], Mingyu Cheng, Nazir Ahmad, Yifan Li, Genqiang Zhang[*]

Hefei National Research Center for Physical Sciences at the Microscale, CAS Key Laboratory of Materials for Energy Conversion, Department of Materials Science and Engineering, University of Science and Technology of China, Hefei 230026, Anhui, China.
[#]These authors contributed equally to this work,

[*]**Correspondence to:** Genqiang Zhang, Hefei National Research Center for Physical Sciences at the Microscale, CAS Key Laboratory of Materials for Energy Conversion, Department of Materials Science and Engineering, University of Science and Technology of China, Hefei 230026, Anhui, China. E-mail: gqzhangmse@ustc.edu.cn

批注 [o1]: Please provide the title for the corresponding author such as "Prof." or "Dr.".

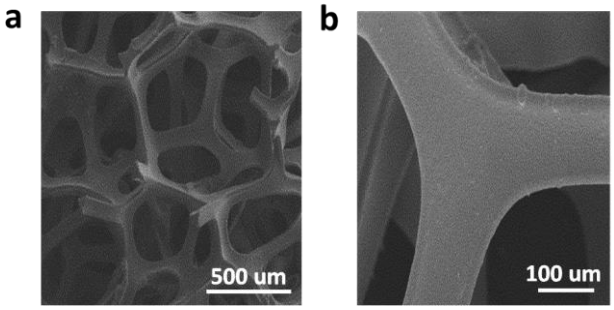

Figure S1. (a-b) SEM images of bare Ni foam.

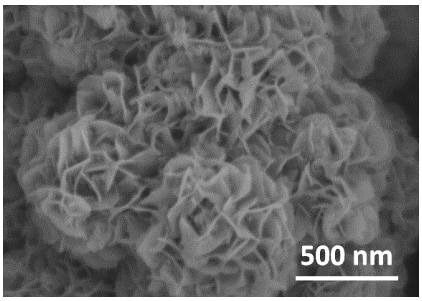

Figure S2. High-magnification SEM image (500 nm scale) of S,W-$Co(OH)_2$/NF showing the detailed nanosheet morphology.

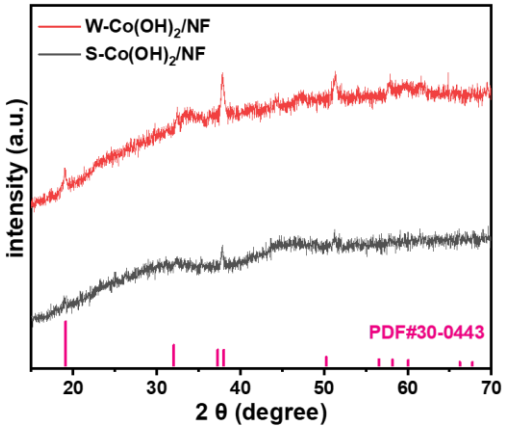

Figure S3. XRD pattern of S-$Co(OH)_2$/NF and W-$Co(OH)_2$/NF.

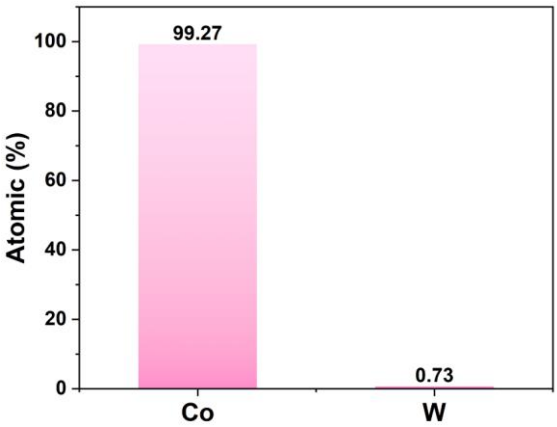

Figure S4. ICP results of S,W-$Co(OH)_2$/NF

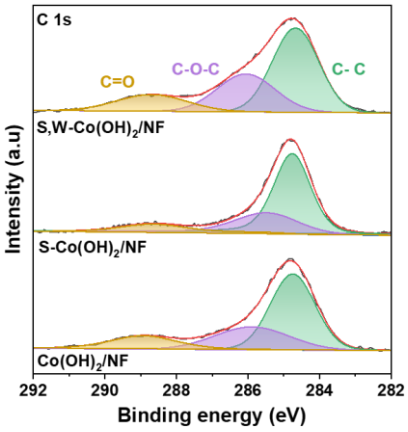

Figure S5. C1s XPS spectrum of $Co(OH)_2$/NF, S-$Co(OH)_2$/NF and S,W-$Co(OH)_2$/NF

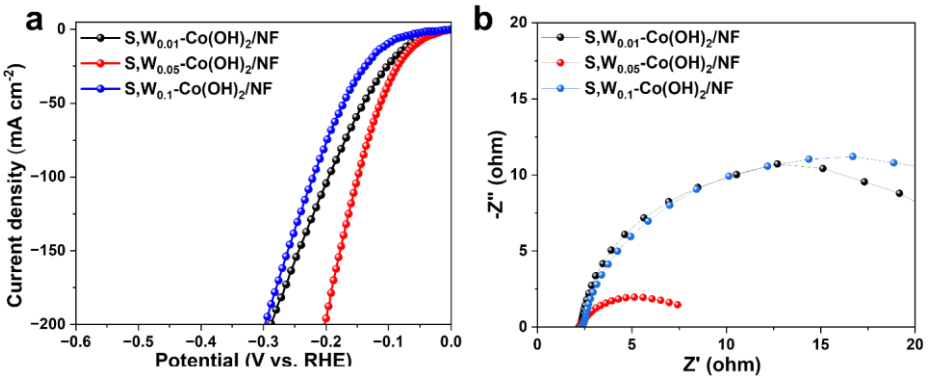

Figure S6. (a) HER Polarization curves and (b) corresponding Nyquist plots for S,W_X-$Co(OH)_2$/NF synthesized at different concentrations of W. (X=0.01, 0.05, and 0.1).

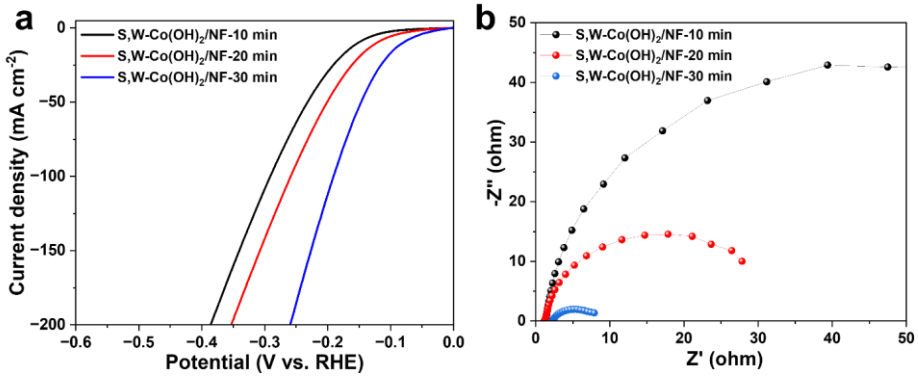

Figure S7. (a) HER polarization curves and (b) corresponding Nyquist plots for S,W-$Co(OH)_2$/NF synthesized at different electrodeposition times.

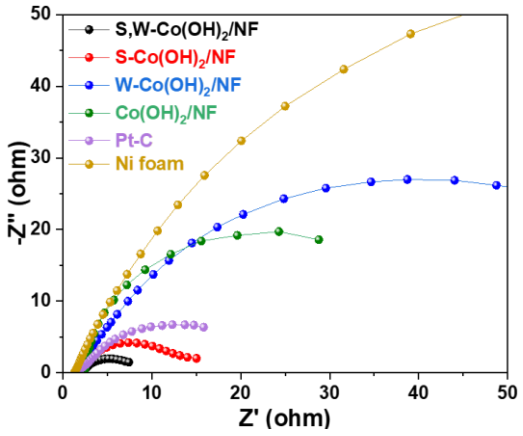

Figure S8. Nyquist plots of various catalysts for the HER process at -0.98 V *vs*. RHE.

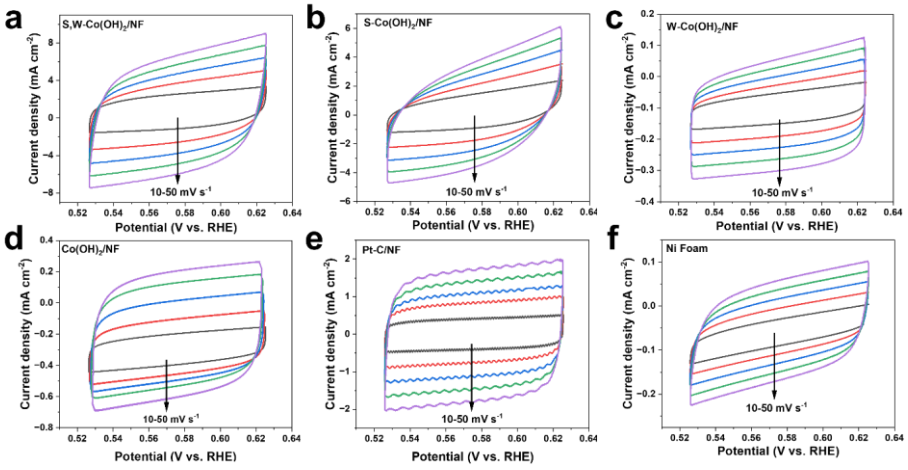

Figure S9. The CV curves of the catalysts were measured with the scan rate from 10 to 50 mV s^{-1} in 1.0 M KOH.

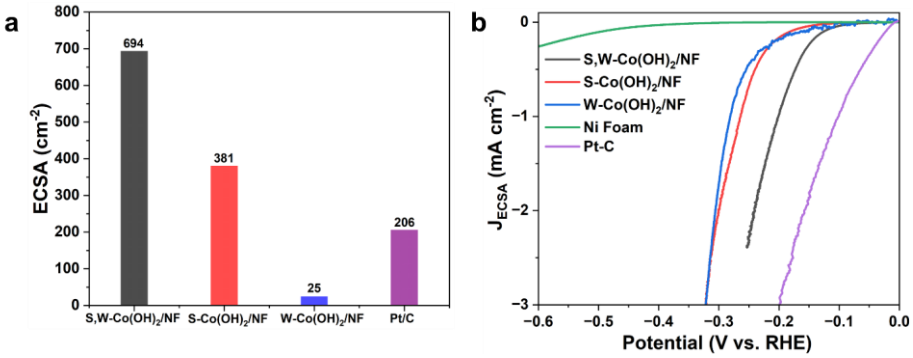

Figure S10. (a) The evaluation of ECSA for different catalysts and (b) corresponding ECSA normalized HER polarization curves.

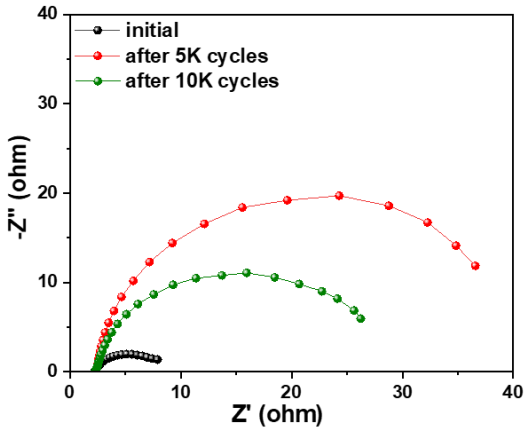

Figure S11. Nyquist plots for HER after X-cycles (X= 5000 and 1000 CV cycles).

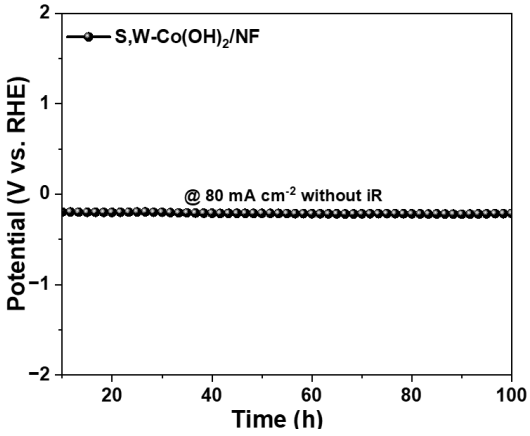

Figure S12. Galvanostatic measurement of long-term stability for HER.

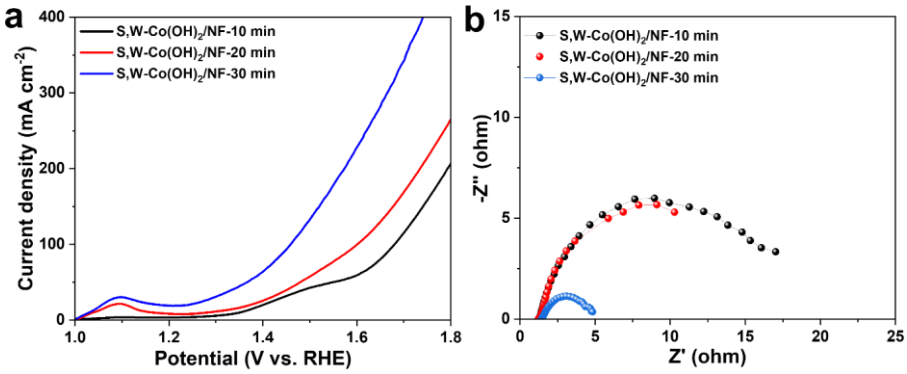

Figure S13. (a) UOR polarization curves and (b) corresponding Nyquist plots for S,W-$Co(OH)_2$/NF synthesized at different electrodeposition times.

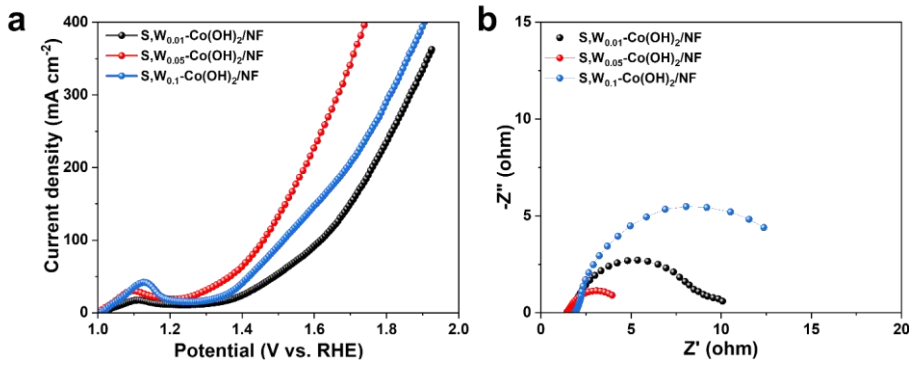

Figure S14. (a) UOR Polarization curves and (b) corresponding Nyquist plots for S,Wx-$Co(OH)_2$/NF synthesized at different contents of W. (X=0.01, 0.05, and 0.1).

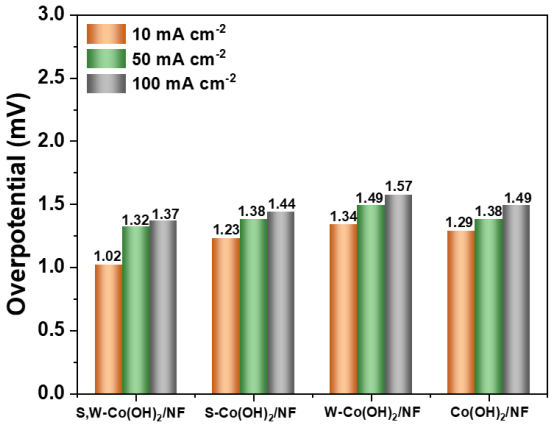

Figure S15. UOR overpotential comparison at 10,50 and 100 mA cm^{-2}.

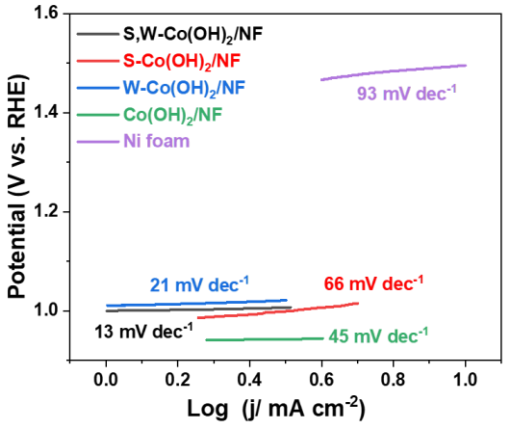

Figure S16. Corresponding Tafel plots of various catalysts for UOR.

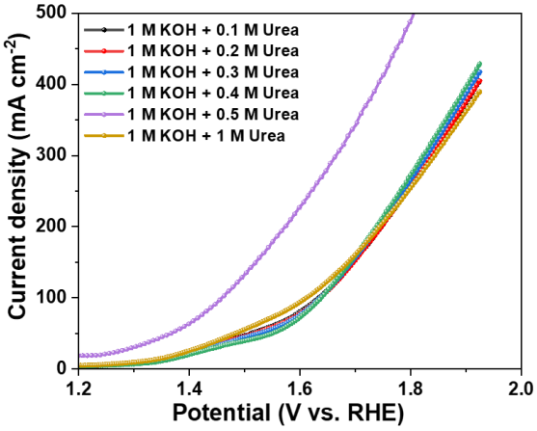

Figure S17. LSV analysis of S,W-Co(OH)$_2$/NF with different concentrations of urea.

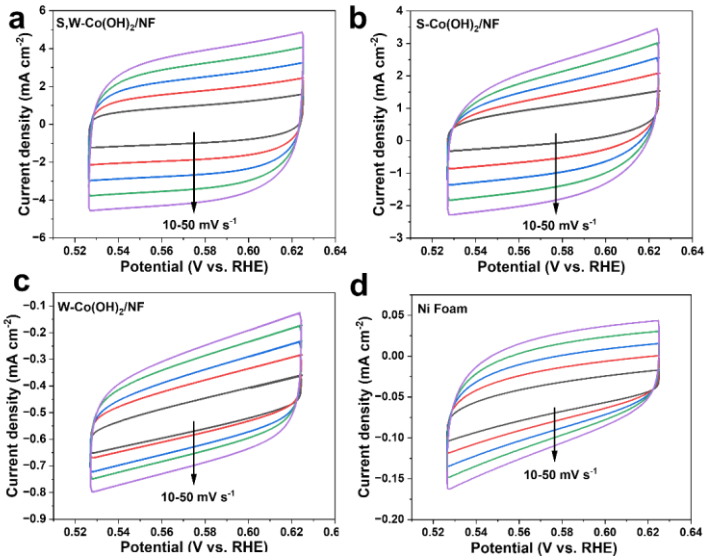

Figure S18. The CV curves of the catalysts were measured with the scan rate from 10-50 mV s^{-1} in 1.0 M KOH + 0.5 M urea.

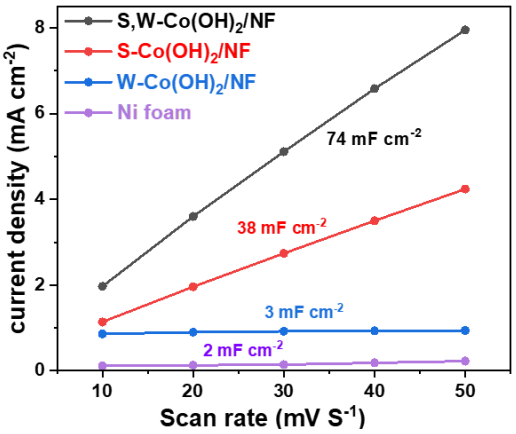

Figure S19. The corresponding C_{dl} values at a potential of 0.57 V *vs*. RHE.

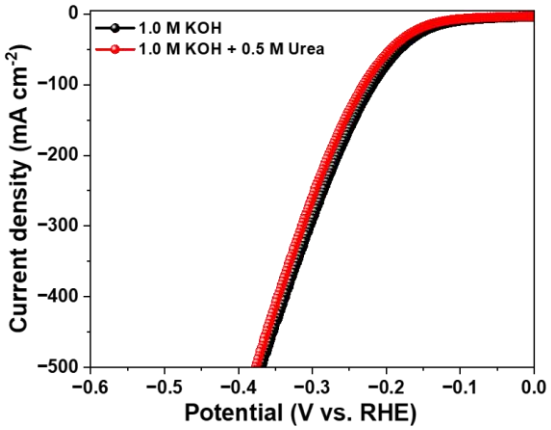

Figure S20. HER polarization curves of S,W-Co(OH)$_2$/NF electrode in 1 M KOH with or without 0.5 M urea.

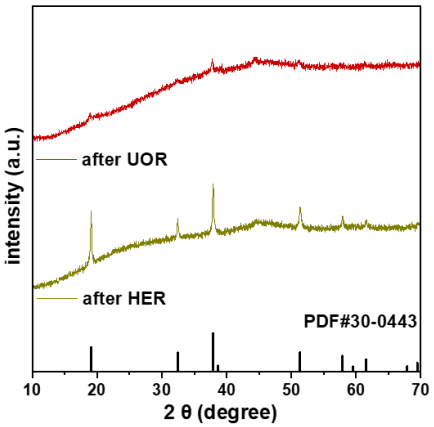

Figure S21. XRD pattern of S,W-Co(OH)$_2$/NF Post-HER and Post-UOR.

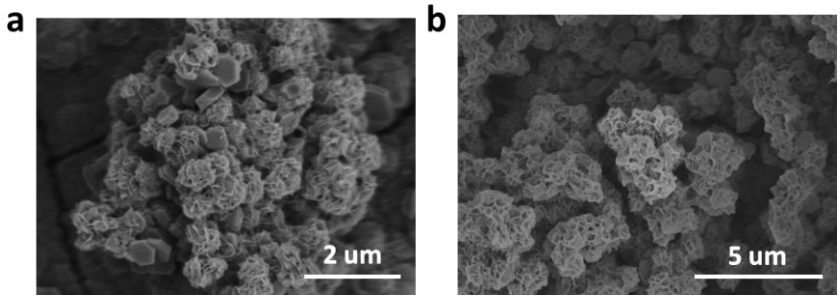

Figure S22. SEM images of S,W-Co(OH)$_2$/NF. (a) Post-HER and (b) Post-UOR Performance test.

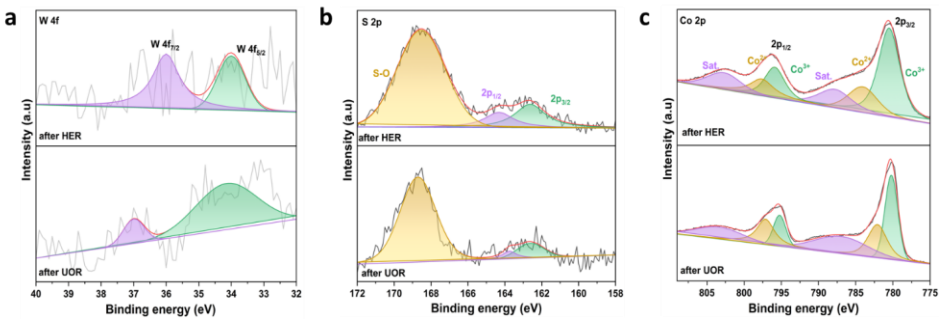

Figure S23. The XPS spectra of S,W-Co(OH)$_2$/NF after performance test, (a) W 4f (b) S 2p, and Co 2p.

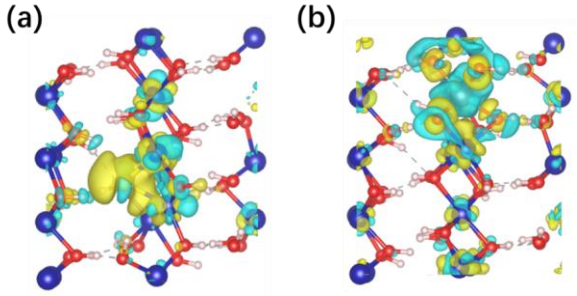

Figure S24. Differential charge density of (a) S-$Co(OH)_2$ and (b) W-$Co(OH)_2$.

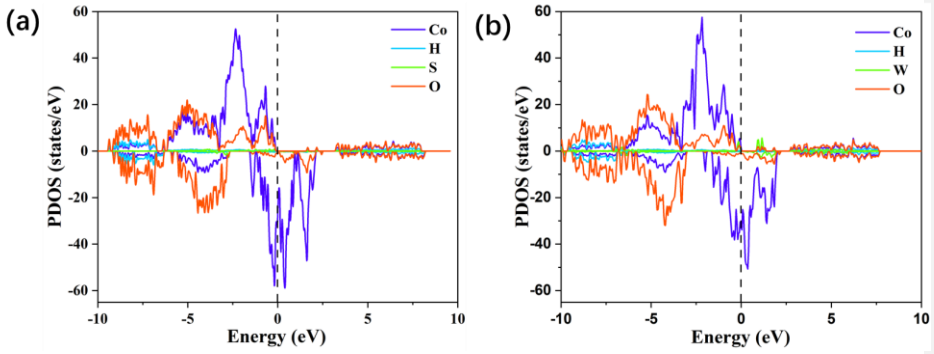

Figure S25. Calculated DOS of (a) S-$Co(OH)_2$ and (b) W-$Co(OH)_2$.

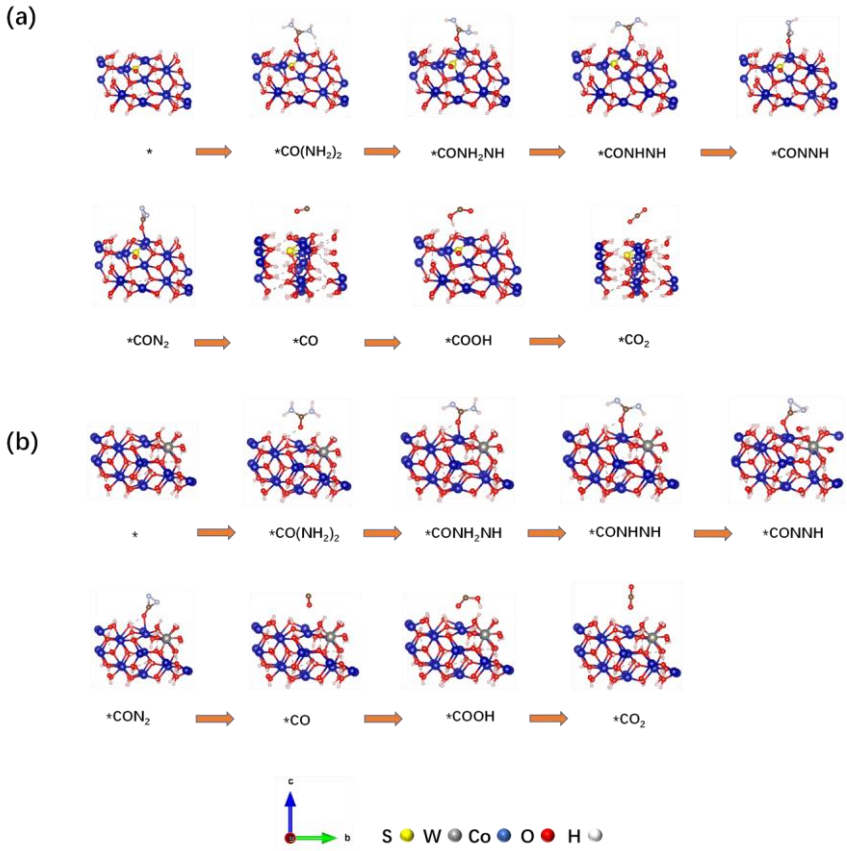

Figure S26. Optimization models for adsorption of different intermediate of $Co(NH_2)_2$ reaction on (a) S-$Co(OH)_2$ and (b) W-$Co(OH)_2$.

Table S1. ICP data.

Sample	Co (%)	W (%)
Bulk S,W-$Co(OH)_2$	99.27%	0.73%

Post-HER S,W-$Co(OH)_2$	99.45%	0.55%
Post-UOR S,W-$Co(OH)_2$	99.22%	0.78%

Table S2. Comparison of the HER performance of S,W-$Co(OH)_2$/NF with the reported catalysts in 1.0 M KOH solution

Materials	**Electrolyte**	**η_{10} (mV)**	**Stability duration / mA cm^{-2}**	**Ref.**
S,W-$Co(OH)_2$/NF	**1.0 M KOH**	**70**	**100 h / 80**	**This work**
Co_xMo_yS-CC	1.0 M KOH	85	24 h / 10	[1]
$Ni_5P_4/CePO_4$/NF	1.0 M KOH	94	10 h / 20	[2]
NiCoFeP/C	1.0 M KOH	149	10 h / 10	[3]
$Fe_{0.86}Ni_{0.14}$-PO_x/CC	1.0 M KOH	125	100 h / 10	[4]
V-$Co_2P_4O_{12}$/CC	1.0 M KOH	109	190 h / 10	[5]
Ni_3S_2/NiCo LDH	1.0 M KOH	156	12 h / 100	[6]
N-Co_9S_8/Ni_3S_2	1.0 M KOH	111	20 h / 20	[7]
NiS/MoS_2	1.0 M KOH	128	10 h / 100	[8]
Ni_3S_2/VG@NiCo LDHs	1.0 M KOH	110	24 h / 20	[9]
FQD/CoNi-LDH	1.0 M KOH	150	25 h / 10	[10]

Table S3. The comparison of UOR performance between S,W-$Co(OH)_2$/NF and other reported materials.

Materials	Electrolyte	E_{10} (V)	Stability duration / mA cm^{-2}	Ref.
S,W-$Co(OH)_2$/NF	**1.0 M KOH+0.5 M Urea**	**1.02**	**100 h / 80**	**This work**
N-Co_9S_8/Ni_3S_2	1.0 M KOH+0.5 M Urea	1.27	20 h / 20	[7]
NiFeCo LDH/NF	1.0 M KOH+0.33 M Urea	0.38	50 h / 10	[11]
S-Co_2P@Ni_2P	1.0 M KOH+0.5 M Urea	1.31	20 h/ 50	[12]
V-$Co_2P_4O_{12}$/CC	1.0 M KOH+0.33 M Urea	1.29	230 h / 10	[5]
$Ni_{0.864}Co_{0.136}$LDH	1.0 M KOH + 0.5 M Urea	1.30	35 h / 70	[13]
NiCoP/CC	1.0 M KOH+0.5 M Urea	1.30	30 h / 20	[14]
CoNi@CNCoNiMoO	1.0 M KOH+0.5 M Urea	1.29	120 / 500	[15]
FeCuCoNiZnLDH/CC	1.0 M KOH+0.33 M Urea	1.32	70 h / 20	[16]
$NiSe_2$/$MoSe_2$	1.0 M KOH+0.33 M Urea	1.33	10 h / 10	[17]

Table S4. Comparison of different catalysts for urea-assisted electrolysis.

Materials	Electrolyte	E_{10} (mV)	Stability duration / mA cm^{-2}	Ref.
S,W-$Co(OH)_2$/NF	**1.0 M KOH+0.5 M Urea**	**1.19**	**24 h / 100**	**This work**
V-$FeNi_3N$/Ni_3N	1.0 M KOH+0.5 M Urea	1.46	15 h / 100	[18]

NiFe/NiFeCH/CC	1.0 M KOH+0.5 M Urea	1.39	30 h / 10	[19]
CoNiFeS-OH/NF	1.0 M KOH+0.5 M Urea	1.46	10 h / 10	[20]
$NiCo_2S_4$NS/CC	1.0 M KOH+0.5 M Urea	1.49	20 h / 10	[21]
Ni_3S_2-Ni_3P/NF	1.0 M KOH + 0.5 M Urea	1.43	100 h / 16	[22]
$NiCo_2S_4$	1.0 M KOH+0.5 M Urea	1.45	10 h / 10	[23]
NiS/MoS_2	1.0 M KOH+0.5 M Urea	1.46	25 h / 10	[24]
FQD/CoNi-LDH	1.0 M KOH+0.5 M Urea	1.45	50 h / 10	[10]
Ni_3N/$Ni_{0.2}Mo_{0.8}N$	1.0 M KOH+0.33 M Urea	1.34	500 h / 10	[25]
Ni_3S_2-H_2|Ni_3S_2-Ar	1.0 M KOH+0.33 M Urea	1.50	20 h / 20	[26]

References

1. Li, P., et al., Insights into the Mo-doping effect on the electrocatalytic performance of hierarchical $Co_x Mo_y S$ nanosheet arrays for hydrogen generation and urea oxidation. ACS applied materials & interfaces, 2020. **12**(36): p. 40194-40203. DOI: https://dx.doi.org/10.1021/acsami.0c10489
2. Liang, Y., et al., Crystalline Ni_5P_4/amorphous $CePO_4$ core/shell heterostructure arrays for highly-efficient electrocatalytic overall water splitting. Journal of Colloid and Interface Science, 2024. **655**: p. 565-575. DOI: https://dx.doi.org/10.1016/j.jcis.2023.11.036
3. Wei, X., et al., Carbon-incorporated porous honeycomb NiCoFe phosphide nanospheres derived from a MOF precursor for overall water splitting. Chemical Communications, 2019. **55**(73): p. 10896-10899. DOI: https://dx.doi.org/10.1039/C9CC06042A

4. Wang, L., et al., Interface engineering of porous nickel-iron phosphates with enriched oxygen vacancies as an efficient bifunctional electrocatalyst for high current water splitting. Electrochimica Acta, 2023. **443**: p. 141932. DOI: https://dx.doi.org/10.1016/j.electacta.2023.141932

5. Chang, X.W., et al., Tuning morphology and electronic structure of cobalt metaphosphate via vanadium-doping for efficient water and urea splitting. Advanced Functional Materials, 2024. **34**(21): p. 2313974. DOI: https://dx.doi.org/10.1002/adfm.202313974

6. Jia, L., et al., Ni_3S_2/Cu–NiCo LDH heterostructure nanosheet arrays on Ni foam for electrocatalytic overall water splitting. Journal of Materials Chemistry A, 2021. **9**(48): p. 27639-27650. DOI: https://dx.doi.org/10.1039/D1TA07523A

7. Xie, H., et al., Construction of nitrogen-doped biphasic transition-metal sulfide nanosheet electrode for energy-efficient hydrogen production via urea electrolysis. Small, 2023. **19**(17): p. 2207425. DOI: https://dx.doi.org/10.1002/smll.202207425

8. Zheng, Y., et al., POM derived UOR and HER bifunctional NiS/MoS_2 composite for overall water splitting. Journal of Solid State Chemistry, 2020. **292**: p. 121644. DOI: https://dx.doi.org/10.1016/j.jssc.2020.121644

9. Zhang, X., et al., Bridging NiCo layered double hydroxides and Ni_3S_2 for bifunctional electrocatalysts: The role of vertical graphene. Chemical Engineering Journal, 2021. **415**: p. 129048. DOI: https://dx.doi.org/10.1016/j.cej.2021.129048

10. Feng, Y., et al., Decorating CoNi layered double hydroxides nanosheet arrays with fullerene quantum dot anchored on Ni foam for efficient electrocatalytic water splitting and urea electrolysis. Chemical Engineering Journal, 2020. **390**: p. 124525. DOI: https://dx.doi.org/10.1016/j.cej.2020.124525

11. Babar, P., et al., Bifunctional 2D electrocatalysts of transition metal hydroxide nanosheet arrays for water splitting and urea electrolysis. ACS Sustainable Chemistry & Engineering, 2019. **7**(11): p. 10035-10043. DOI: https://dx.doi.org/10.1021/acssuschemeng.9b01463

12. Yuan, W., et al., Interface engineering of S-doped Co_2P@ Ni_2P core–shell heterostructures for efficient and energy-saving water splitting. Chemical Engineering Journal, 2022. **439**: p. 135743. DOI: https://dx.doi.org/10.1016/j.cej.2022.135743

13. Zheng, Z., et al., Collaborative optimization of thermodynamic and kinetic for Ni-based hydroxides in electrocatalytic urea oxidation reaction. Applied Catalysis B: Environmental, 2024. **340**: p. 123214. DOI: https://dx.doi.org/10.1016/j.apcatb.2023.123214
14. Sha, L., et al., The construction of self-supported thorny leaf-like nickel-cobalt bimetal phosphides as efficient bifunctional electrocatalysts for urea electrolysis. Journal of Materials Chemistry A, 2019. **7**(15): p. 9078-9085. DOI: https://dx.doi.org/10.1039/C9TA01876E
15. Qian, G., et al., Strong electronic coupling of CoNi and N-doped-carbon for efficient urea-assisted H2 production at a large current density. Carbon Energy, 2023. **5**(12): p. e368. DOI: https://dx.doi.org/10.1002/cey2.368
16. Hao, M., et al., Lattice-disordered high-entropy metal hydroxide nanosheets as efficient precatalysts for bifunctional electro-oxidation. Journal of Colloid and Interface Science, 2023. **642**: p. 41-52. DOI: https://dx.doi.org/10.1016/j.jcis.2023.03.042
17. Yin, C., et al., Heterostructured $NiSe_2/MoSe_2$ electronic modulation for efficient electrocatalysis in urea assisted water splitting reaction. Chinese Journal of Catalysis, 2023. **51**: p. 225-236. DOI: https://dx.doi.org/10.1016/S1872-2067(22)64178-5
18. Wang, J., et al., Vanadium-doping and interface engineering for synergistically enhanced electrochemical overall water splitting and urea electrolysis. ACS Applied Materials & Interfaces, 2021. **13**(48): p. 57392-57402. DOI: https://dx.doi.org/10.1021/acsami.1c16789
19. Wang, X., et al., Cauliflower-like NiFe alloys anchored on a flake iron nickel carbonate hydroxide heterostructure towards superior overall water and urea electrolysis. Nanoscale, 2023. **15**(2): p. 779-790. DOI: https://dx.doi.org/10.1039/D2NR05789A
20. Fang, C., et al., In situ growth of S-incorporated CoNiFe (oxy) hydroxide nanoarrays as efficient multifunctional electrocatalysts. Inorganic Chemistry Frontiers, 2022. **9**(14): p. 3643-3653. DOI: https://dx.doi.org/10.1039/D2QI00654A
21. Zhu, W., et al., Traditional NiCo2S4 phase with porous nanosheets array topology on carbon cloth: a flexible, versatile and fabulous electrocatalyst for overall water and urea electrolysis. ACS Sustainable Chemistry & Engineering, 2018. **6**(4): p. 5011-5020. DOI: https://dx.doi.org/10.1021/acssuschemeng.7b04665
22. Liu, J., et al., Heterostructured Ni_3S_2–Ni_3P/NF as a bifunctional catalyst for overall urea–water electrolysis for hydrogen generation. ACS Applied Materials & Interfaces, 2021. **13**(23): p. 26948-26959. DOI: https://dx.doi.org/10.1021/acsami.1c04662

23. Song, W., et al., Construction of self-supporting, hierarchically structured caterpillar-like NiCo 2 S 4 arrays as an efficient trifunctional electrocatalyst for water and urea electrolysis. Nanoscale, 2021. **13**(3): p. 1680-1688. DOI: https://dx.doi.org/10.1039/D0NR07964A
24. Gu, C., et al., NiS/MoS2 Mott-Schottky heterojunction-induced local charge redistribution for high-efficiency urea-assisted energy-saving hydrogen production. Chemical Engineering Journal, 2022. **443**: p. 136321. DOI: https://dx.doi.org/10.1016/j.cej.2022.136321
25. Li, R.-Q., et al., Hierarchical $Ni_3N/Ni_{0.2}Mo_{0.8}N$ heterostructure nanorods arrays as efficient electrocatalysts for overall water and urea electrolysis. Chemical Engineering Journal, 2021. **409**: p. 128240. DOI: https://dx.doi.org/10.1016/j.cej.2020.128240
26. Zhang, Y., et al., Coaxial Ni–S@ N-doped carbon nanofibers derived hierarchical electrodes for efficient H2 production via urea electrolysis. ACS Applied Materials & Interfaces, 2021. **13**(3): p. 3937-3948. DOI: https://dx.doi.org/10.1021/acsami.0c19873